How to Cite:
Abdul-Salam, M., & Tawfeeq , N. A. (2022). Biological activity against breast cancer cells of iron(II), copper(II) & nickel(II) complexes with Di-m-bromobenzalcyclohexanone & dibenzalcyclohexanone - thiosemicarbazide schiff bases. *International Journal of Health Sciences*, *6*(S9), 1139–1153. https://doi.org/10.53730/ijhs.v6nS9.12432

Biological activity against breast cancer cells of iron(II), copper(II) & nickel(II) complexes with Di-m-bromobenzalcyclohexanone & dibenzalcyclohexanone - thiosemicarbazide schiff bases

Maryam Abdul-Salam
Department of Chemistry, College of Education for Pure Sciences, University Of Al-Anbar, Ramadi, Iraq
Email: mah20s3009@uoanbar.edu.iq

Nabeel Arif Tawfeeq
University of Anbar, College of Education for Women, Department of Chemistry, Ramadi, Anbar, Iraq.
Email: edw.nobel_ani_70@uoanbar.edu.iq

***Abstract*---**The title work included synthesis of new symmetrical dibenzalcyclohexanone substituted with one bromine group at meta position of each benzene ring. The synthesised ketones were dibenzalcyclohexanone and di-m-bromobenzalcyclohexanone. Di-m-bromobenzalcyclohexanone was synthesised through the reaction of cyclohexanone with benzaldehyde in the presence of potassium hydroxide, as well as the preparation of ketones substituted with bromine at meta position from the reaction of cyclohexanone with the substituted benzaldehyde at meta position. The synthesised chalcones were characterized using different spectral and physical techniques. These ketones were used to prepare new Schiff bases by reacting the thiosemicarbazide compound with the previously mentioned un-substituted chalcone, first ligand, while the second ligand was prepared by reacting the meta-bromobenzalcyclohexanone with thiosemicarbazide. The synthesised ligands were bi-dentate ligand, according to this matter six metal complexes were synthesised through reacting two moles of Schiff bases with one mole of nickel (II), iron (II), & copper (II) chlorides. The novel metal complexes were characterized by different techniques such as ^{1}H&^{13}C-NMR and mass spectrometry (Mass Spectra) in addition to measurements of magnetic susceptibility and molar conductivity of the prepared complexes. Through spectroscopic studies and magnetic susceptibility, and physical properties, the shape of the prepared complexes were

International Journal of Health Sciences ISSN 2550-6978 E-ISSN 2550-696X © 2022.
Manuscript submitted: 9 May 2022, Manuscript revised: 18 July 2022, Accepted for publication: 27 August 2022

predicted. The iron and copper complexes are paramagnetic complexes, and the magnetic moment values are within the range of the distorted tetrahedral shape. For nickel complexes, they are diamagnetic complexes, and the magnetic moment values are within the range of the distorted square-planar shape. These suggestions agreed with previous studies of similar systems. The biological activity of the prepared complexes against breast cancer cell line MDA-MB231 was evaluated. The results showed that the three metal complexes had activity against cancer cells with a concentration less than (50) micromolar. Nickel complex with meta-substituted Schiff base showed moderate activity with IC_{50} value equal to 31.9 micromolar. Copper complex with dibenzalcyclohexanone-thiosemicarbazide showed also moderate activity better than the previous nickel complex with IC_{50} equal to 24.3 micromolar. While the best activity was for iron complex with meta-bromobenzalcyclohexanone with a value of IC_{50} equal to 16 µmolar. From these results, we expect that the preparation of metal complexes from Schiff bases replaced by more than one bromine group will certainly lead to obtaining compounds with very strong efficacy against cancer cells, especially breast cancer type MDA-MB 231.

***Keywords*---**Breast Cancer, Metal Complexes, Biological Activity, Schiff Bases.

1 Introduction

1.1 Anti-cancer chalcones

Cancer diseases of all kinds are considered among the widespread diseases that man suffers from at the present time, and it is a disease that is widespread in all parts of the world. All researchers in this field are motivated to develop new therapeutic agents in the field of cancer detection and treatment of cancerous diseases. All countries and organizations are pushing Annually large sums of money in research related to this field [1] . As it is known, anti-cancer drugs are effective drugs in the treatment of cancerous or malignant diseases. Some of them are intended for the treatment of certain types of cancer, and some of them are a general treatment for the treatment of different types. Medication, which leads to a decrease in the clinical efficacy of anti-cancer drugs, and the severe side effects of chemotherapeutic agents reduce the clinical efficacy of a large variety of commonly used anti-cancer agents, and therefore there is always an ongoing need to develop alternative anti-cancer drugs with minimal side effects [2]. It was observed that the complexes of divalent and tetravalent platinum and divalent palladium with chalcones [3-4] showed good efficacy against human cancer cells [5] .

2 Materials and Methods

2.1 Ketones Synthesis

In Becker, mix 2.325 g of cyclohexanone and 14.9 g of 3-bromobenzaldehyde dissolved in 100 ml of ethanol with stirring by a glass stirrer. An aqueous solution

of potassium hydroxide consisting 4 grams of potassium hydroxide in 20 ml of distilled water was gradually added to the mixture with stirring for half an hour. A yellowish precipitate was formed, then 50 ml of cold distilled water was added to the mixture with stirring for a quarter of an hour. The mixture was filtered, recrystallization was carried out with ethanol, and the resulting precipitate was left to dry to obtain a clean, dry precipitate. The resulting substance is yellow in color, its weight is (13.89) grams, and its melting point is (110-113 °C)[6].

2.2 Schiff base Synthesis

In a round bottom flask, 7.84 g of di-m-bromobenzalcyclohexanone dissolved in 50 ml ethanol and 1.82 g of thiosemicarbazide dissolved in 25 ml of ethanol were also placed in a flask. (10-15) drops of hydrochloric acid were added gradually as a catalyst for the reaction during the escalation of the mixture for a period of 3 hours. The solution was cooled, filtered and left to dry. Re-crystallization was done using absolute ethanol to obtain a pure precipitate. Color (yellow), weight (8.69) grams, and melting point (120-122) °C [7].

2.3 Metal Complexes Synthesis

In a circular flask, dissolve 1.5 g of Schiff base in 100 ml of ethanol with stirring and heating. Heat in a second baker 0.45 g of the metal salt dissolved in 50 mL of ethanol. Nickel salt was added to the Schiff base gradually. Leave the mixture to rise for an hour to obtain a precipitate. Then filter the solution and leave to dry to give a precipitate[8].

3 Results and Discussions

pr Schiff bases were prepared from the reaction of thiosemicarbazide with chalcones that were prepared from the reaction of brominated cyclohexanone at meta position. While metal complexes were synthesised by reacting metal salts and Schiff base with a ratio of (1:2) metal to ligands. The molar electrical conductivity of the metal complexes was measured at a concentration of (10^{-3} M) in dimethylsulfoxide after allowing the solution to be in equilibrium at 25°C. It was found that the complexes were classified as having a neutral non-electrolytic (non-ionic) behavior. The following table shows the molar electrical conductivity values of the complexes prepared in this study.

Table (1)
Molar Conductivity of the Synthesised Metal Complexes

No	Complex	Cod. μ $S.cm^2.mole^{-1}$	Type of complex
1	$[Cu(L1)_2]$	12	Non-electrolyte
2	$[Cu(L2)_2]$	12	Non-electrolyte
3	$[Ni(L1)_2]$	2	Non-electrolyte
4	$[Ni(L2)_2]$	2	Non-electrolyte
5	$[Fe(L1)_2]$	10	Non-electrolyte
6	$[Fe(L2)_2]$	0	Non-electrolyte

3.1 Magnetic Susceptibility Measurement

Magnetic susceptibility measurement is widely used in studying and diagnosing transition metal complexes. After applying the calculations and comparing the practical results of the magnetic susceptibility values with the theoretical results, the results showed that the iron and copper complexes are paramagnetic complexes and that the magnetic moment values fall within the special range of the distorted tetrahedron, while the nickel complexes are diamagnetic complexes and that the values of The magnetic moment is within the range of the distorted plane square shape [8]. The following table shows the magnetic susceptibility values.

Table (2)
Magnetic Susceptibility of the Synthesised Metal Complexes & the Predicted Geometry

No	Complex	μ_{eff} (BM) calculated	μ_{eff} (BM) found	Suggested Geometry
1	$[Ni(L_1)_2]$	0	0	Distorted square planar
2	$[Ni(L_3)_2]$	0	0	Distorted square planar
3	$[Cu(L_1)_2]$	1.73	1.49	Distorted tetrahedral
4	$[Cu(L_3)_2]$	1.73	1.49	Distorted tetrahedral
5	$[Fe(L_1)_2]$	1.73 (Fe^{3+})	1.49	Distorted tetrahedral
6	$[Fe(L_3)_2]$	4.9	4.8	Distorted tetrahedral

3.2 Physical Properties (State, Color & Melting Point)

The following table shows the most important measured physical properties of the resulting materials that were prepared in this study, as it is clear from the table that the resulting materials differ greatly from the reactants, which indicates the formation of new materials that differ from the raw materials.

Table (3)
Physical Properties of Reactants and Products

Melting Point (°C)	Color	Physical State	Compound
88-90	orange	Solid	DBC-TSC(L1)
120-122	yellow	Solid	D-3-BrBC-TSC(L2)
122-124	light red	Solid	Ni-$(L1)_2$
159d	Dark brown	Solid	Cu-$(L1)_2$
179-182	Dark red	Solid	Fe-$(L1)_2$
139-140	green	Solid	Ni-$(L2)_2$
219-220	brouwn	Solid	Cu-$(L2)_2$

134-136	light red	Solid	Fe-(L2) $_2$

3.3 UV-Visible Spectra of Metal Complexes

3.3.1 Ultraviolet-visible spectra of the first ligand complexes L $_1$

The UV-visible spectrum of the nickel complex [Ni(L1) $_2$] showed absorption peaks at wavelengths (300,335, & 341) due to the π →π * and n →π * electronic transitions. transition) and the reason for this is that all electrons in orbital (d) are paired and there are no single electrons in it . Figure (1) shows the UV-visible spectrum of a nickel complex with an uncompensated Schiff base with a bromine group (L 1).

Also, the UV-visible spectrum of the complex $[Cu(L1)_2]$, Fig.(2), showed an absorption peak (315 nm) (31746cm^{-1}) that belongs to the π→π * and n→π * electron transitions, as well as An absorption band whose peak is at the wavelength (617 nm), which is due to a transition known as (dd transition) ^{2} B $_1$ → ^{2} A $_1$ and this transition is attributed to the tetrahedral shape. As for the UV-visible spectrum, Fig. (3), it showed two peaks of the complex $[Fe(L1)_2]$ at the range (301-342 nm) (33222-29239cm^{-1}), which are due to the π→π* electronic transitions to the peak (301 nm) and n→π* returns to the top (342 nm) and returns the band whose peak is at the wavelength (625 nm), it goes back to the type (d-d transition) of electronic transitions $^5E\rightarrow {}^5T_2$ and these transitions are attributed to the figure. The geometric tetrahedron and the table (4) and Figure No. (3) illustrate this.

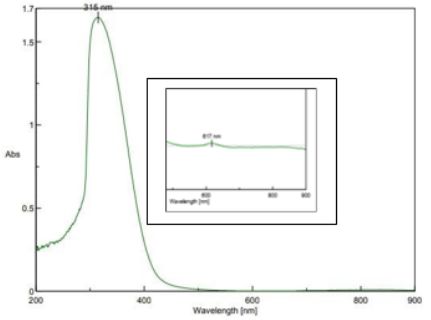

Figure(2): UV-visible spectrum of the complex $[Cu(L1)_2]$

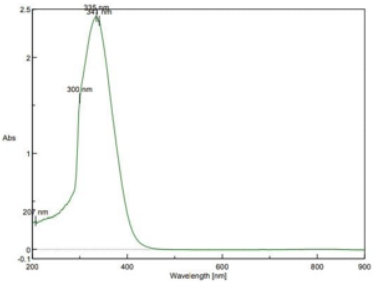

Figure(1): UV-visible spectrum of the complex $[Ni(L1)_2]$

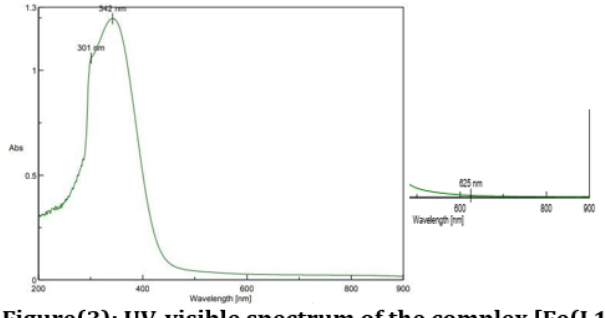

Figure(3): UV-visible spectrum of the complex $[Fe(L1)_2]$

3.3.2 UV-visible spectra of Metal Complexes of (L2) ligand

The UV-visible spectrum of nickel complexes [Ni(L2)$_2$], Fig. (4), showed absorption peaks at the range (304-331 nm) (32894-30211cm^{-1}) that belong to the π→π* electronic transitions. For the peak (304 nm) and n→π* for the peak (331 nm). We also note that there are no absorption bands specific to the d-d transition. This is due to the duplication of all electrons in orbital (d) and the absence of single electrons in it. Because of this, the geometric shape of the nickel complex is expected to be a distorted square-planar shape or square planar)[1]. As for the ultraviolet spectrum of the complex [Cu(L2)$_2$], Figure No. (5), it showed one absorption peak at wavelength 305,335 nm) (32787-29851cm^{-1}) due to the electronic transitions π→π* and n→π* as well as an absorption band whose peak is at the wavelength (765 nm), which refers to the type of transition (d-d transition) $^2B_1 \rightarrow {}^2A_1$ and this transition is attributed to the tetrahedral shape. Also, the ultraviolet spectrum of the complex [Fe(L2)$_2$], Figure (6), showed several peaks at the range (325-341 nm) (30769-29325cm^{-1}), which are due to the π→π* electronic transitions for the peak pick at wavelength equal to 325nm and n →π* for the peak pick at wavelength equal to 341nm and the charge transitions at 405 nm and the band that reached its peak at the wavelength 616 nm belongs to d-d transition of electronic transitions $^5E \rightarrow {}^5T_2$ These transitions are attributed to the tetrahedral geometric shape and Table (4) and Figure No. (6) illustrate this.

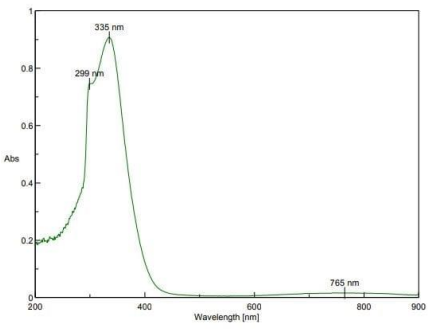

Figure(5): UV-visible spectrum of the complex [Cu(L2)$_2$]

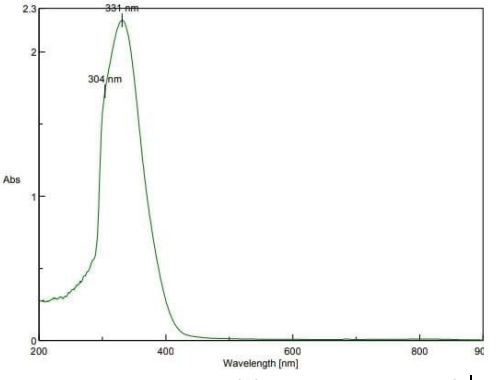

Figure(4): UV-visible spectrum of the complex [Ni(L2)$_2$]

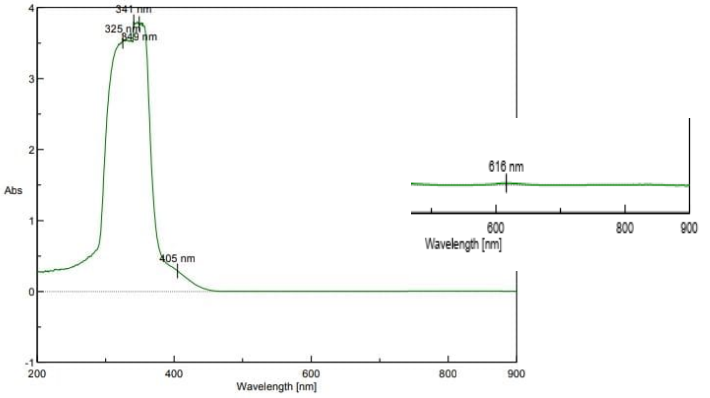

Figure(6): UV-visible spectrum of the complex [Fe(L2)$_2$]

Table 4
The most important spectral peaks and bands of the UV-visible spectrum of the prepared compounds

Complex	λ (nm)	υ (cm^{-1})	Assignment	Proposed Structure
L1	300 335	33333 29850	π→π * n →π *	------
L2	330	30303	n →π *	------
$[Ni(L1)_2]$	300 335 341	33333 29850 29325	π→π * n →π * n →π *	Distorted square planar
$[Ni(L2)_2]$	304 331	32895 30211	π→π * n →π *	Distorted square planar
$[Cu(L1)_2]$	315 617	31746 16207	n →π * d-d transition $^2B_1 \rightarrow {}^2A_1$	Distorted tetrahedral
$[Cu(L2)_2]$	305 335 765	32787 29850 13072	π→π * n →π * d-d transition $^2B_1 \rightarrow {}^2A_1$	Distorted tetrahedral
$[Fe(L1)_2]$	301 342 625	33222 29239 16000	π→π * n →π * d-d transition $^5E \rightarrow {}^5T_2$	Distorted square planar
$[Fe(L2)_2]$	325 341 349 616	30769 29235 28653 16234	π→π * n →π * CT d-d transition $^5E \rightarrow {}^5T_2$	Distorted tetrahedral

3.4 Infrared Spectra (FT-IR)
3.4.1 Infrared Spectra (FT-IR) for Schiff bases

The prepared compounds were spectroscopically characterized by FT-IR spectrum. Figures (7) and (8) for the prepared compounds (Schiff bases) indicated the disappearance of the stretchable vibration absorption bands of the (νC=O) ketone group, And the appearance of the elastic vibration absorption bands of azomethine group (νC=N) in the range (1599-1602cm^{-1}), in addition to the appearance of the stretchable vibration absorption bands ($\nu C\text{-}H_{arom}$) within the range (3155-3147cm^{-1}) that the appearance of these bands It is considered a preliminary guide for the correctness of the working method used in preparing these compounds, and Table No. (5) shows the values of the absorption beams of the infrared spectrum FT-IR for the prepared compounds (Schiff bases):

Table 5
Shows the values of the absorption bands of the infrared spectrum FT-IR for compounds (Schiff bases) measured in cm $^{-1}$

Comp. Symb.	νC-H Arom.	νC-H Aliph.		C=S	νC=N	ν C=C$_{ring}$		Others
		Asym.	Sym.					
DBC-TSC	3147	2936	2861	1075.7	1599	599	1489	NH $_2$ and NH 3433, 3255
3-Br-DBC-TSC	3150	2935	2863	1079	1602	1595	1471	NH $_2$ and NH 3430, 3256 C-Br at 784

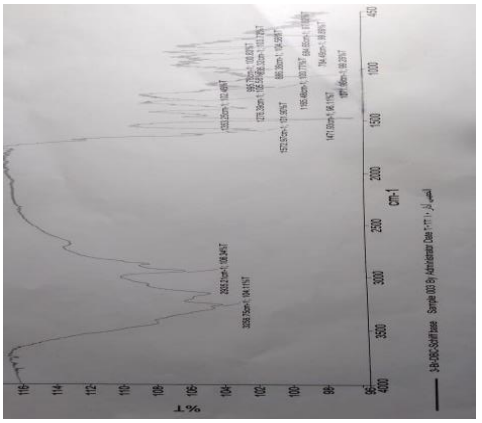

Figure (8): FT-IR spectrum of 3-Br-DBC-TSC Schiff Base

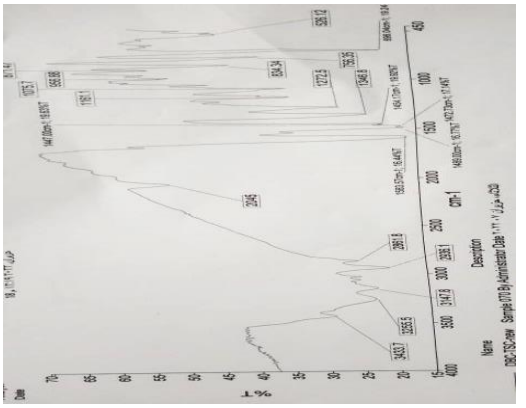

Figure (7): FT-IR spectrum of DBC-TSC Schiff Base

3.4.2 FT-IR Spectra of Complexes

The prepared compounds were spectroscopically characterized by FT-IR spectrum. Figures (9) to (14) for the prepared compounds (metal complexes) indicated the appearance of the stretch-vibration absorption bands of azomethene group (νC=N) at the range (1664-1606cm^{-1}), in addition to the appearance of the bands of stretching vibration absorption (νC-H$_{arom}$) within the range (3157-3048cm^{-1}). It shows the values of the absorption bands of the FT-IR spectrum of the prepared metal complexes:

Table No. (6):
Shows the values of the absorption bands of the infrared spectrum FT-IR for the prepared metal complexes measured in cm^{-1}

Comp. Symb.	νC-H Arom.	νC-H Aliph.		νC=N	ν C=C ring		Others	MN
		Asym.	Sym.					
DBC-Ni	3156	2936	2863	1606	1606	1494	NH_2, 3411,3280	570
3-Br-DBC-Ni	3140	2935	2860	1608	1608	1473	NH 2,3392,3250	539
DBC-Cu	3150	2929	2866	1615	1599	1497	NH_2 3435,3270	565
2-BrDBA-Cu	3140	2929	2870	1632	1599	1466	NH_2 3435,3252	527
3-BrDBC-Cu	3088	2961	2917	1632	1605	1441	NH_2 3344,3252	530
DBC-Fe	3090	2918	2850	1628	1599	1474	NH_2 3435,3255	520
2-BrDBC-Fe	3157	2936	2862	1610	1593	1468	NH_2 3402,3278	534
3-BrDBC-Fe	3048	2940	2830	1664	1606	1475	NH_2 3435, 3240	540

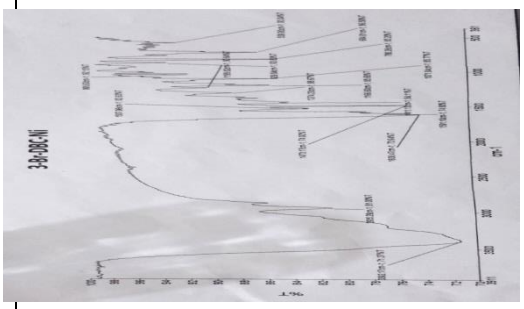

Figure(10): FT-IR Spectrum for 3-Br-DBC-Ni

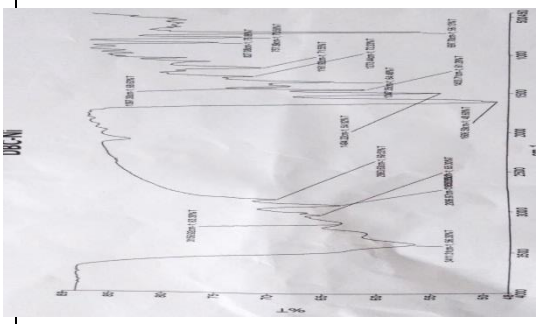

Figure(9): FT-IR Spectrum for DBC-Ni

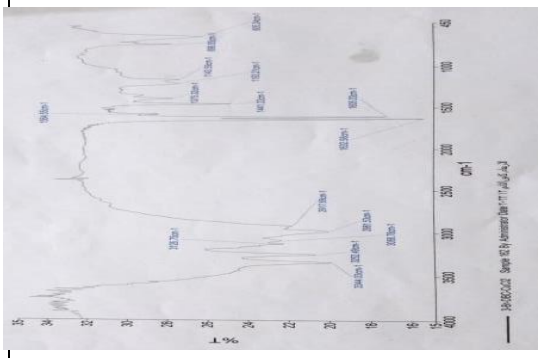

Figure(12): FT-IR Spectrum for 3-Br-DBC-Cu

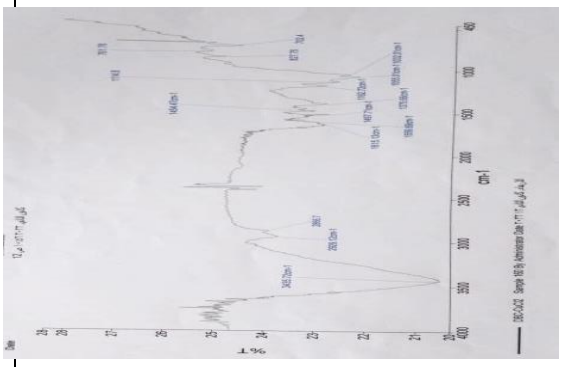

Figure(11): FT-IR Spectrum for DBC-Cu

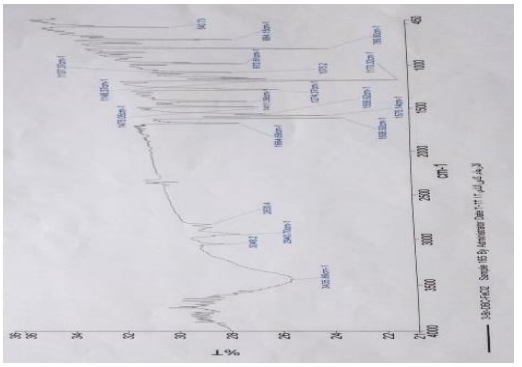

Figure(14): FT-IR Spectrum for 3-Br-DBC-Fe

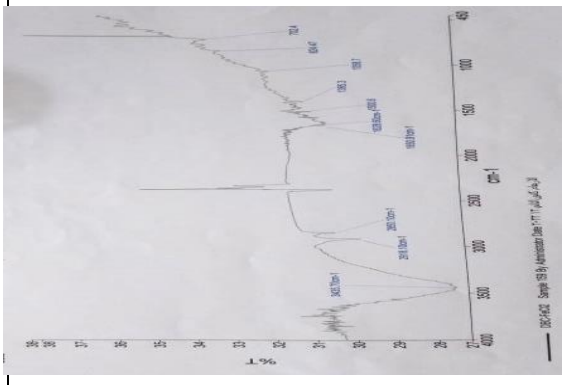

Figure(13): FT-IR Spectrum for DBC-Fe

3.5 NMR Spectra of Complexes

The structural formula of the compounds was also confirmed by the ^{1}H-NMR spectrum of the proton . In general, Figures (15), and (16) indicated the following bands and absorptions. The prepared compound (DBC-Ni Complex), Figure No. (15), showed multiple signals at [δ=(1.62-1.64) ppm, (m,4H)] belonging to the alkane group in the saturated hexagonal ring, and it appeared A triple sign at [δ=(3.09-3.11) ppm,(t,8H)] returns to the two alkane groups of the saturated hexagonal ring, and a single sign at [δ=(6.87) ppm,(s,4H) , =CH = C H] returns to

the alkene group, and a multiple signal appeared at [δ=(7.33-7.46) ppm,(m,20H) , -Ar- H .] belongs to the aromatic ring protons, and shows a single signal at [δ = (9.46) ppm, (s,4H) , -N H_2] belongs to the amine group.

Compound (3-Br-DBC-Ni complex), Figure (16), showed a multi-signal at [δ = (1.62-1.67) ppm, (m,4H)] belonging to the alkane group in the saturated hexagonal ring. And a triple signal appeared at [δ = (33.12-3.14) ppm, (t, 8H)] belonging to the two alkane groups of the saturated hexagonal ring, and a single signal appeared at [δ = (6.55) ppm, (s,4H) , C H =] belongs to the alkene group, and a multiple signal appeared at [δ = (7.31-7.58) ppm, (m, 16H), -Ar- H .] belongs to the aromatic ring protons, and a single signal appeared at [δ = (9.72) ppm, (s,4H), -N H_2] belonging to the amine group. Table No. (3-10) shows the chemical displacement of the compounds (complexes) diagnosed by nuclear magnetic resonance spectroscopy.

Table 7:
The chemical displacement of the compounds (complexes) diagnosed by nuclear magnetic resonance spectroscopy, measured in ppm

Comp. Symb.	Structure	Chemical Shift(ppm)	No. of Protons	Type of signal	Group
$[Ni(L1)_2]$	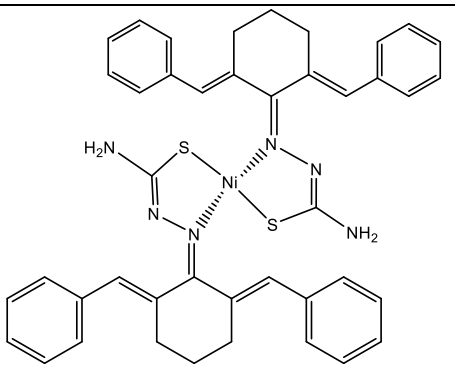	1.61-1.64	4	M	Aliphatic protons
		3.09-3.11	8	T	
		6.87	4	S	C H = C -
		7.33-7.46	20	M	Aromatic Protons
		9.46	4	S	-N H_2
$[Ni(L2)_2]$	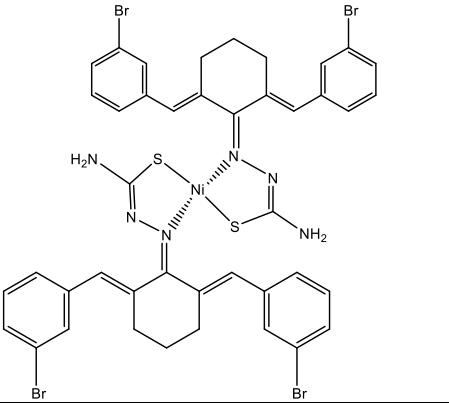	1.62-1.67	4	M	Aliphatic protons
		3.12-3.14	8	T	
		6.55	4	S	C H = C -
		7.31-7.58	16	M	Aromatic Protons
		9.72	4	S	-N H_2

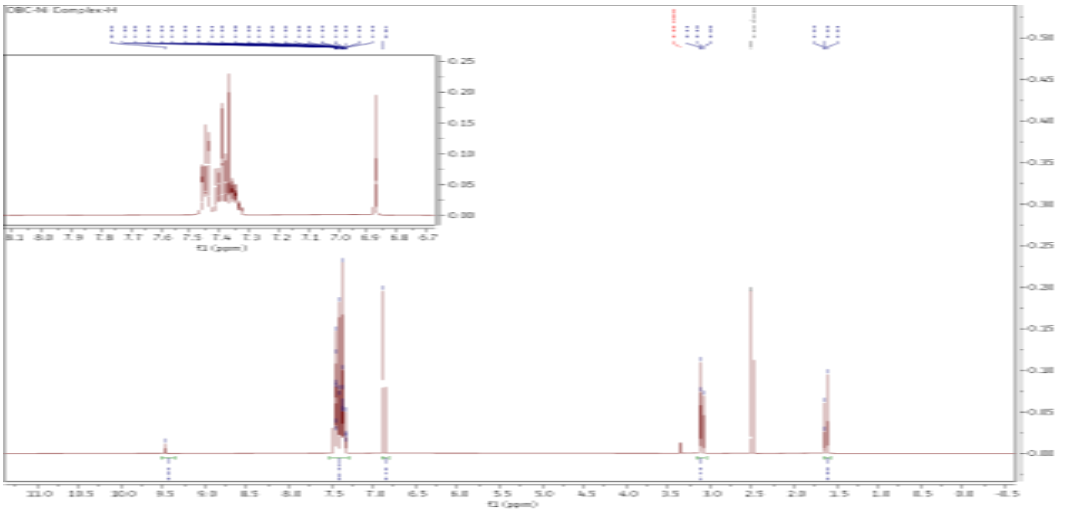

Figure (15): Expanded & condensed [1] H-NMR spectrum of the DBC-Ni Complex

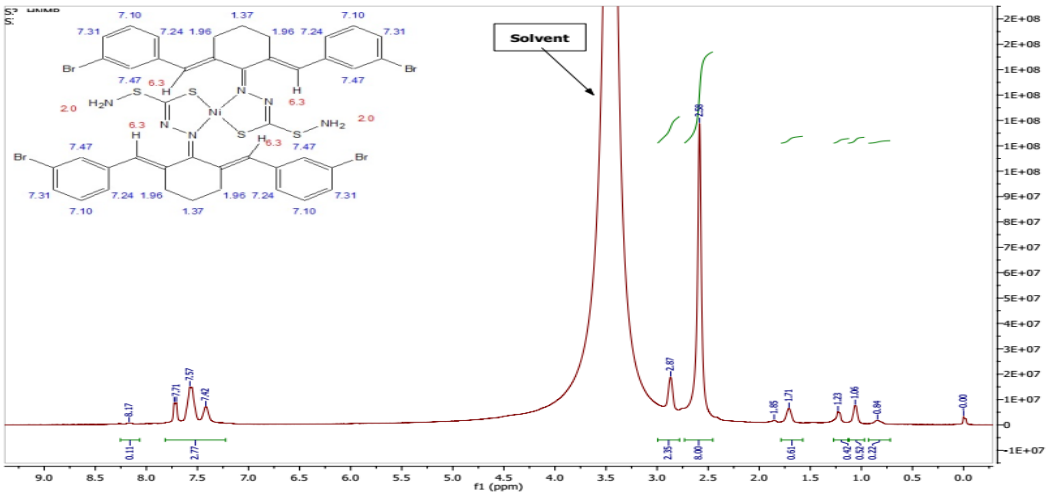

Figure (16): Expanded & condensed [1] H-NMR spectrum of 3-Br-DBC-Ni complex

3.6 Mass spectra

Most of the research and studies concerned with the preparation of ligands and complexes for transition elements depend on mass spectrometry, as it gives clear and confirmed evidence on the structural formulas of the prepared isomethenic compounds and their complexes, by observing the molecular ion bundle (M^+) and the basic bundles of ligands and some of the prepared complexes. The appearance of bundles representing Lc-mass - The results of the Lc-mass diagnosis of ligands and some of the prepared complexes showed the appearance of bands representing the molecular weight, and from that the proposed formulas were validated that are consistent with the results of other measurements. With the proposed formulas that were interpreted as stated in the literature [9,10] .

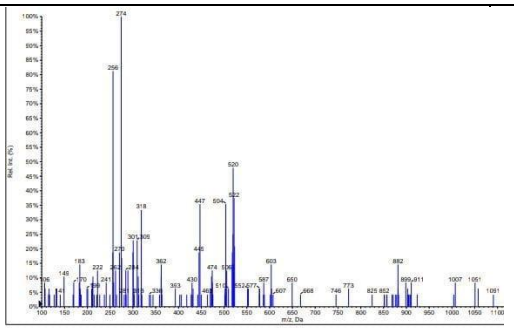

Figure(18): Mass spectrum of 3 -Br-DBC-TSC

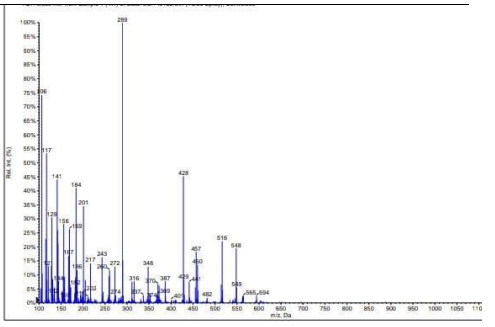

Figure(17): Mass spectrum of DBC-TSC

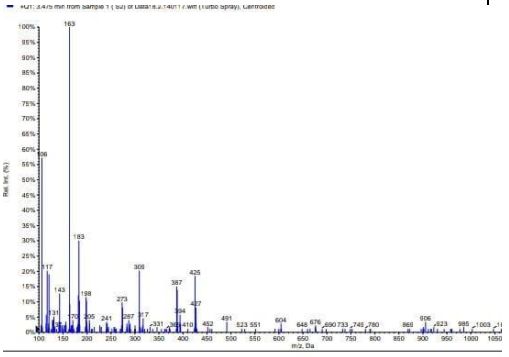

Figure(20): Mass spectrum of the DBC-Cu complex

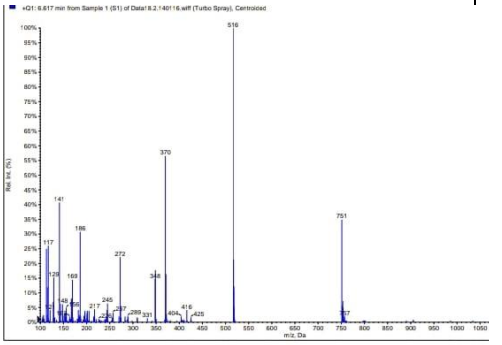

Figure(19): Mass spectrum of the DBC-Ni complex

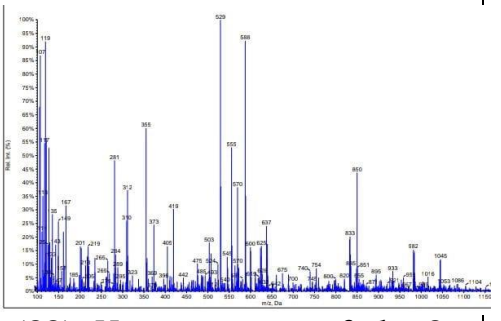

Figure(22): Mass spectrum of the 3 -Br-DBC-Cu complex

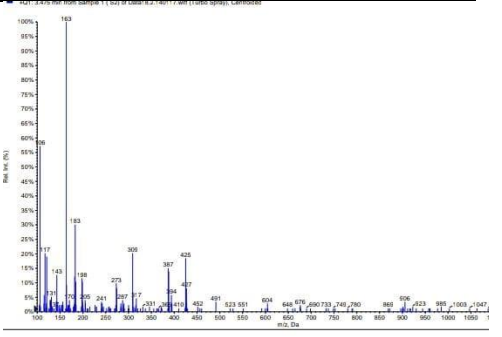

Figure(21): Mass spectrum of the DBC-Fe complex

3.7 Biological activity of the prepared metal complexes

Cancer cells can be defined as that group of cells that escape from the normal growth process of the various cells of the human body and then work on developing their ability to change the rest of the normal cells of the tissue or organ in the human body. Breast cancer is one of the types of cancerous diseases that affect females in a very large proportion, as well as affecting men less than females. It is worth noting that one of the most important challenges facing the process of treating diseases or cancer cells is the ability and ability of cancer cells

to resist treatment or medication, as it works to find a new resistance or mechanism to resist and overcome the drug, so the drug used or prepared must have two important characteristics The first is an anti-resistance property and the second is that the drug is multi-purpose for the purpose of overcoming the drug-resistant property of cancer cells. Where the drug binds to the DNA of cancer cells, and this connection works to make the DNA curve uneven, which leads to the inhibition of RNA synthesis.

Based on the foregoing, this study aims to prepare an effective drug or treatment against cancer cells in general and against breast cancer cells in particular. The effectiveness of the prepared metal complexes was studied for the first time in this study against breast cancer cells using the well-known method, the MTT method. It is known that breast cancer cells are of several types. In this study, one type of breast cancer cell, MDA-MB 231, was studied and the effect of the metal complexes prepared for the first time was studied. The IC_{50} was measured for each of the nine complexes using certain concentrations of the dissolved complexes. In the solvent DimethylSulfoxide (DMSO) which acts as a good solvent for complexes as well as a negative standard material (Negative Control). Table No. 8 shows the efficacy of the metal complexes prepared in this study against breast cancer cells of MDA-MB 231 type, and IC_{50} values for each of the complexes.

Table 8:
Cytotoxicity of Metal Complexes against Breast Cancer Cell Line MDA-MB231

IC_{50}	Metal Complexes
>50µM	Ni-DBC-TSC
24.3µM	Cu-DBC-TSC
>50µM	Fe-DBC-TSC
31.9µM	Ni-m-Br-DBC-TSC
>50µM	Cu-m-Br-DBC-TSC
16µM	Fe-m-Br-DBC-TSC

From the table it is clear that three metal complexes have been effective against cancer cells With a concentration of less than (50) micromolar, the nickel complex with a substituted Schiff base with a bromine group in the dead site has a value of (IC_{50} = 31.9) micromolar and the copper complex with an uncompensated Schiff base with any active group with a value of (IC_{50} = 24.3) micromolar and the best of the best is the iron-binary complex consistent with a base The offset with a bromine group in the dead site has a value of (IC_{50} = 16) µmol.

4 Conclusion

From these results, we expect that the preparation of metal complexes from Schiff bases replaced by more than one bromine group will certainly lead to obtaining compounds with very strong efficacy against cancer cells, especially breast cancer type MDA-MB 231.

References

1. Altman, L. K. (1997). A growing threat: cancer. *Positively aware: the monthly journal of the Test Positive Aware Network*, *8*(4), 21-23.
2. Arianggara, A. W., Ernawati, E., Handayani, T. P., Sari, F., & Fitria, L. (2022). Relationship of information sources and knowledge with completeness of primigravida's tetanus toxoid immunization. International Journal of Social Sciences and Humanities, 6(1), 75–84. https://doi.org/10.53730/ijssh.v6n1.4738
3. Fu, D. J., Zhang, S. Y., Liu, Y. C., Zhang, L., Liu, J. J., Song, J., ... & Zhang, Y. B. (2016). Design, synthesis and antiproliferative activity studies of novel dithiocarbamate–chalcone derivates. *Bioorganic & medicinal chemistry letters*, *26*(16), 3918-3922.
4. Gaber, M., El-Ghamry, H. A., & Mansour, M. A. (2018). Pd (II) and Pt (II) chalcone complexes. Synthesis, spectral characterization, molecular modeling, biomolecular docking, antimicrobial and antitumor activities. *Journal of Photochemistry and Photobiology A: Chemistry*, *354*, 163-174.
5. Gross, J. H. (2006). *Mass spectrometry: a textbook*. Springer Science & Business Media.
6. Huang, X., Huang, R., Wang, Z., Li, L., Gou, S., Liao, Z., & Wang, H. (2018). Pt (IV) complexes conjugating with chalcone analogue as inhibitors of microtubule polymerization exhibited selective inhibition in human cancer cells. *European Journal of Medicinal Chemistry*, *146*, 435-450.
7. Islam, M. A. A. A. A., Sheikh, M. C., Mahmud, A. A., Miyatake, R., & Zangrando, E. (2016). Benzyl 3-(3, 4, 5-trimethoxybenzylidene) dithiocarbazate. *IUCrData*, *1*(2), x160190.
8. Nurman, D. G., Karim, A. K., Akhnazarov, S. K., Mukashev, S. T., & Demissenov, O. M. (2021). Current issues of molecular diagnostics of bladder cancer. International Journal of Health Sciences, 5(3), 286–301. https://doi.org/10.53730/ijhs.v5n3.1477
9. Silverstein, R. M., & Bassler, G. C. (1962). Spectrometric identification of organic compounds. *Journal of Chemical Education*, *39*(11), 546.
10. Suryasa, I. W., Rodríguez-Gámez, M., & Koldoris, T. (2021). Get vaccinated when it is your turn and follow the local guidelines. International Journal of Health Sciences, 5(3), x-xv. https://doi.org/10.53730/ijhs.v5n3.2938
11. Tawfeeq, N. A.(2019). Synthesis of transition metal complexes containing symmetrical chalcone-derived Schiff bases and cytotoxic studies against bladder cancer cells - Universiti Putra Malaysia Institutional Repository. http://psasir.upm.edu.my/id/eprint/83237/. Accessed July 22, 2022.
12. Vanchinathan, K., Bhagavannarayana, G., Muthu, K., & Meenakshisundaram, S. P. (2011). Synthesis, crystal growth and characterization of 1, 5-diphenylpenta-1, 4-dien-3-one: An organic crystal. *Physica B: Condensed Matter*, *406*(22), 4195-4199.
13. Xu X, Qiu G, Ji L, Ma R, Dang Z, Jia R, et al. Research and development of anticancer agents under the guidance of biomarkers. Cancer Traditional Medicine. 2019;5(1):17-21